Thermal noise of whispering-gallery resonators

Akobuije Chijioke, Qun-Feng Chen, Alexander Yu. Nevsky, and Stephan Schiller*
Institut für Experimentalphysik, Heinrich-Heine-Universität Düsseldorf, 40225 Düsseldorf, Germany
(Received 27 June 2011; published 11 May 2012)

By direct application of the fluctuation-dissipation theorem, we numerically calculate the fundamental thermal fluctuations of the dimensions of crystalline CaF_2 whispering-gallery resonators in the case of structural damping, and the limit that this noise imposes on the frequency stability of such resonators at both room and cryogenic temperatures. We analyze elasto-optic noise—the effect of Brownian dimensional fluctuation on frequency via the strain-dependence of the refractive index—a noise term that has so far not been considered for whispering-gallery resonators. We find that dimensional fluctuation sets a lower limit of 10^{-16} to the Allan deviation for a 10-mm-radius sphere at 5 K, predominantly via induced fluctuation of the refractive index.

DOI: 10.1103/PhysRevA.85.053814 PACS number(s): 42.60.Da, 05.40.Jc, 06.30.Ft

I. INTRODUCTION

The properties of a body in equilibrium at a finite temperature undergo continuous fluctuation about their mean values. The fluctuation-dissipation theorem of Callen and Welton [1] established the relationship between these fluctuations and the dissipative properties of the system. This fundamental relationship is of great practical importance in precision measurements, such as the measurement and stabilization of the frequency of laser light using high-quality-factor optical cavities. Thermal noise sets a limit on the frequency stability of optical cavities, and hence on their performance in such applications.

The thermal noise of conventional Gaussian-mode optical cavities has been analyzed in detail [2–5], providing guidance in the design of such cavities. A relatively new type of high-finesse optical cavity is the whispering-gallery resonator (WGR) [6], in which light is confined inside an axially symmetric dielectric object by continuous-total-internal reflection. Solid dielectric optical WGRs were quickly recognized as potentially useful [7] due to their high quality factors and small mode volumes, resulting in an intense confined coherent optical field. The lowest cavity loss demonstrated so far resulted in a linewidth of about 1 kHz in pure crystalline CaF_2 [8], making these resonators very attractive candidates for precision laser frequency stabilization. Understanding thermal noise in such resonators is critical for this application. For a WGR, both the fluctuation of the radius and of the refractive index must be considered. We present a calculation, by direct application of the fluctuation-dissipation theorem, of the frequency instability due to fundamental thermal fluctuation of the dimensions of crystalline CaF_2 resonators.

Initial estimates of thermal noise in WGRs have been made [9,10], in particular for thermorefractive noise, the fluctuation of the refractive index due to fundamental temperature fluctuations. The thermorefractive noise has recently been measured for crystalline resonators at room temperature [11]. The thermal noise due to fundamental dimensional fluctuations at a fixed temperature has been less investigated. For laser frequency stabilization, the fluctuations on time scales of 0.01 s to hundreds of seconds are of interest for applications such as clock lasers for optical clocks [12] or tests of fundamental symmetries such as Lorentz invariance [13]. We find that at low temperatures the thermal noise due to dimensional fluctuation dominates over the thermal noise due to fundamental temperature fluctuation. We find that the dominant component of the dimensional-fluctuation thermal noise is due to induced changes of the refractive index, via the elasto-optical effect.

To calculate the thermal noise we follow the direct approach introduced by Levin [3] for standard two-mirror resonators, adapting it to WGRs. We perform the calculations numerically, by finite-element analysis, for sphere- and disk-shaped resonators.

II. CALCULATION

A. Temperature fluctuation

Our calculations reported in this paper are focused on the fundamental dimensional fluctuations that occur at a fixed temperature. However, to determine the expected dominant thermal noise terms in different regimes and to make contact with existing thermal noise results for WGRs, we compare our calculated noise levels to thermal noise arising from fundamental temperature fluctuations at a given mean temperature. These cause whispering-gallery mode (WGM) frequency fluctuation via the dependence of refractive index on temperature (thermorefractive noise, TR) and thermal expansion of the resonator (thermoelastic noise). We evaluate the thermorefractive noise of a sphere using the expression of Gorodetsky and Grudinin [10],[1]

$$S_{df/f} = \frac{8k_B T^2 \Gamma(R,f,T)}{\pi^2 \gamma(T) R} \left(\frac{1}{n}\frac{dn}{dT}\right)^2, \tag{1}$$

$$\sigma_{\mathrm{TR}}(\tau) = \frac{2T}{\pi}\sqrt{\frac{k_B \Gamma(R)}{\gamma(T) R \tau}} \left(\frac{1}{n}\frac{dn}{dT}\right), \tag{2}$$

where Γ evaluates to 0.847 for a 1-mm-radius CaF_2 sphere at low frequency and for the entire temperature range of interest, and γ is the thermal conductivity. We expect the thermoelastic noise to be small relative to the thermorefractive noise, as the volume over which temperature fluctuations are averaged

*step.schiller@uni-duesseldorf.de

[1]This is the discrete sum expression (A15) of Ref. [10], the applicable expression for low frequencies.

is much larger in the case of thermoelastic noise, while the thermal expansion and thermorefractive coefficients are of similar magnitude.

B. Brownian boundary noise

The fluctuation-dissipation theorem says that the power spectral density of fluctuations of coordinate x of a body, at frequency f is

$$S_x(f) = \frac{k_B T}{\pi^2 f^2} |\mathrm{Re}[Y(f)]|, \tag{3}$$

where $Y(f) = 2\pi i f x(f)/F(f)$ is the susceptibility for displacement $x(f)$ under action of the force conjugate to it, $F(f)$. Levin [3] noted that

$$|\mathrm{Re}[Y(f)]| = \frac{2W_{\mathrm{diss}}(f)}{F^2}, \tag{4}$$

where W_{diss} is the dissipation when an oscillating force of magnitude F conjugate to the desired displacement and of frequency f is applied. The cycle-averaged dissipation can be written as

$$W_{\mathrm{diss}}(f) = 2\pi f U(f) \phi(f,T), \tag{5}$$

where U is the strain energy in the body at the temporal maximum of the applied force and $\phi(f,T)$ is the loss angle of the material.[2] We assume that ϕ is constant with respect to frequency (structural damping). The constant loss-angle model is supported by experimental measurements on ultralow-expansion material (ULE) Fabry-Perot cavities in the frequency range 1 Hz down to 3 mHz [2]. We thus have

$$S_x(f) = \frac{4}{\pi} \frac{k_B T U(f) \phi(T)}{f F^2} \tag{6}$$

$$\rightarrow S_{dR/R}(f) = \frac{4}{\pi} \frac{k_B T U \phi(T)}{R^2 f F^2}, \tag{7}$$

where in (7) we have specialized to the case $x = R$ and divided by the radius squared to get the spectral density of relative radius fluctuations, and the f dependence of U has been dropped (static approximation). Since the relative change of the WGR eigenmode frequency ν with mode radius R is $d\nu/\nu = dR/R$,[3] the Allan deviation of the relative resonance frequency fluctuations for this $1/f$ spectrum is independent of integration time,

$$\sigma_{\mathrm{BB}} = \left[\frac{8\ln(2)}{\pi}\right]^{1/2} \frac{\sqrt{k_B T U \phi(T)}}{RF}. \tag{8}$$

We refer to this type of thermal noise as "Brownian boundary" (BB) noise.

Thus, to calculate the fluctuation of the mode path length, we apply an oscillating force conjugate to a stretching of this path. This is a force along the circumferential optical path in the interior of the resonator, with a transverse spatial distribution identical to the mode intensity profile. A circumferential (ring) load is elastically equivalent to a radial one.[4] As the mode is very close to the surface of the resonator, the load can be closely approximated by a surface radial stress distribution with the profile of the one-dimensional (radial) integral of the mode profile. This is the load that we apply.

The calculation is carried out in two steps. First, the electromagnetic field of a fundamental whispering-gallery mode [chosen to be at $\sim 1.9152 \times 10^{14}$ Hz (1565 nm) for concreteness] is simulated using the PDE module of the finite-element package COMSOL,[5] using weak-form partial differential equations following the procedure of Oxborrow [14,15]. The field intensity along the vertical midline of a 2D cross section of the mode is then fit by a Gaussian. The field intensity distribution in the radial direction is also fitted for use in the elasto-optic calculation described in the next subsection. These fitted profiles are the desired information from the electromagnetic simulation.

The second step is to calculate the strain energy stored in the resonator when a load with the same profile as the electromagnetic mode intensity is applied to the resonator surface. We do this for a resonator with its axis along the [111] crystal direction, and in the static approximation (i.e., material acceleration is neglected), accurate for low-frequency noise. The calculation is carried out using COMSOL's 3D structural mechanics module. The strain energy is integrated over the body to give U and the applied load is integrated over the surface to give F.[6] Equation (8) then furnishes the Allan deviation. In both the electromagnetic and strain-energy simulations, care is taken to mesh sufficiently densely in the mode region. In the strain energy simulation, the deformation patterns observed corresponded well to the applied load profiles, indicating that the force magnitudes used were sufficient. Numerical values of CaF_2 properties used in the calculation are listed in Appendix A.

C. Elasto-optic noise

The dimensional fluctuation of the resonator also affects the mode frequency indirectly via the the elasto-optic effect, the dependence of the refractive index on strain. Relative fluctuations of different points in the resonator material correspond to fluctuating strains, and the refractive index of the material varies with strain as described by its elasto-optic coefficients [16]. We refer to this type of thermal noise as "elasto-optic" (EO) noise. This noise term has also recently been considered for multilayer mirror coatings in Fabry-Perot cavities [17]. The effect of the fluctuation of strain component ϵ on the Allan deviation can be written as

$$\sigma_{\mathrm{EO}} = \frac{1}{\nu}\left(\sigma_\epsilon \frac{\partial \nu}{\partial n}\frac{\partial n}{\partial \epsilon}\right) \simeq \frac{\sigma_\epsilon n^2 p}{2}, \tag{9}$$

[2]We neglect the minor temperature-dependence of material elastic constants, and thus of U. Likewise in the next subsection we neglect the temperature-dependence of elasto-optic coefficients.

[3]The effect of the strain dependence of the refractive index is included in the next subsection; if included here it would cause deviation of this relation from rigorous equality by ~6%.

[4]Static equilibrium of the resonator material implies that a tensile ring load T applied at radial position ρ is necessarily accompanied by a radial compressive load per unit length $X = T/r$.

[5]*COMSOL Multiphysics*, COMSOL, Ab., Tegnergatan 23, SE-111 40 Stockholm, Sweden. Available online: http://www.comsol.com. Version 3.5 used.

[6]F may also be determined by simple analytic integration as $F = (2\pi)^{3/2} A R w$, where the applied Gaussian load is $Ae^{-[z/(\sqrt{2}w)]^2}$.

where p is the elasto-optic coefficient ($p = \frac{\partial(1/\varepsilon)}{\partial\epsilon}$, where ε is the dielectric constant), and we have used the approximation $\frac{\partial\nu}{\partial n} \simeq -\frac{\nu}{n}$, valid for azimuthal mode index $\gg 1$.

As for the BB noise, we calculate σ_ϵ using the direct application of the FDT. To calculate the fluctuation of a given strain component, we apply a load to the resonator conjugate to that strain that is spatially weighted according to the intensity of the mode. We evaluate the strain energy in the resonator resulting from the application of this load, and then obtain the strain fluctuation by using for x in Eq. (6) the dimension corresponding to the strain in question.

In general there are six strain components (ϵ_{11},ϵ_{22},ϵ_{33},ϵ_{12},ϵ_{13},ϵ_{23}) to be considered. We restrict our consideration to volume fluctuations, and we therefore consider only the dilational strain $dV/V = \epsilon_{11} + \epsilon_{22} + \epsilon_{33}$. We expect from the elasto-optic tensor that the effects of shear strain fluctuations will be of similar magnitude. We perform the dilational calculation by writing the volume of the mode as $\sim 2\pi^2 r^2 R$, where r is the mode toroid effective minor diameter. Thus the relative fluctuation of the mode volume is

$$\sigma_{dV/V} = \sigma_{dR/R} + 2\sigma_{dr/r}, \tag{10}$$

$\sigma_{dR/R}$ is given by the calculation of the previous section ($\sigma_{dR/R} = \sigma_{\rm BB}$). We calculate $\sigma_{dr/r}$ by applying a stress distribution $\vec{\Sigma}$ radially directed to the mode center,

$$(\Sigma_\rho, \Sigma_\theta, \Sigma_z) = -\Sigma_0 \frac{I(\rho,z)}{I_0}\left(\frac{\rho-\rho_0}{\sqrt{(\rho-\rho_0)^2+z^2}}, 0, \frac{z}{\sqrt{(\rho-\rho_0)^2+z^2}}\right), \tag{11}$$

$$\frac{I(\rho,z)}{I_0} = \exp\left\{-\left[\left(\frac{\rho-\rho_0}{w_\rho}\right)^2 + \left(\frac{z}{w_z}\right)^2\right]\right\}, \tag{12}$$

where the mode center in cylindrical coordinates (ρ,θ,z) is the circle $(\rho_0,\theta,0)$. Then $\sigma_{dr/r}$ is given by

$$\sigma_{dr/r} = \left[\frac{8\ln(2)}{\pi}\right]^{1/2} \frac{\sqrt{k_B T U \phi(T)}}{r\left[2\pi \int_{\rm WGR} (\Sigma_\rho + \Sigma_z)\, \rho d\rho dz\right]}. \tag{13}$$

For r in the above relation we use the (averaged) Gaussian $1/e$ intensity radius $r = \sqrt{w_\rho w_z}$. The dilational elasto-optic coefficient is given in terms of the Cartesian tensor components by $(p_{11} + 2p_{12})/3$. Thus from Eqs. (10) and (9) we have[7]

$$\sigma_{\rm EO} \simeq \left(\frac{1}{2}\sigma_{dR/R} + \sigma_{dr/r}\right) \frac{p_{11}+2p_{12}}{3} n^2. \tag{14}$$

In our calculations we find that $\sigma_{dr/r}/\sigma_{dR/R}$ ranges from 12 to 160 for the resonator sizes considered, and we therefore neglect the first term in Eq. (14). The contribution of the $\sigma_{dR/R}$ term increases as the WGR size decreases.

[7]The + sign in Eq. (14) is understood to indicate the appropriate combination of the terms taking into account any correlation between them that may be present.

III. SIMPLE ESTIMATES

A. Brownian boundary noise

We can make a simple estimate of the BB noise of a spherical resonator by considering the strain energy that results from a uniform pressure on its surface. We expect that this will yield a noise smaller than the true value for a spherical WGR, as in this estimate the radius fluctuations will be averaged over the entire spherical surface surface rather than over only the mode region. For a sphere subject to a constant surface pressure P the strain energy U is

$$U = P\Delta V = P\frac{VP}{\kappa} = \frac{4\pi}{3}\frac{P^2R^3}{\kappa}, \tag{15}$$

where $\kappa = (C_{11} + 2C_{12})/3$ is the bulk modulus for a cubic crystal with elastic constants C_{11} and C_{12}. The applied force is $F = 4\pi R^2 P$, thus we estimate

$$\tilde{S}_{dR/R}(f) = \frac{1}{3\pi^2}\frac{k_B T\phi(T)}{\kappa R^3 f}, \tag{16}$$

$$\tilde{\sigma}_{\rm BB}(\tau) = \left[\frac{(2/3)\ln(2)}{\pi}\right]^{1/2}\sqrt{\frac{k_B T\phi(T)}{\kappa R^3}}. \tag{17}$$

For a 1-mm-radius sphere at 5.5 K, with $\phi = 2\times10^{-8}$ [18], this gives $\sigma_{\rm BB} = 3\times10^{-17}$ for CaF_2 ($\kappa = 90$ GPa), a factor of 2.5 smaller than the value determined by more detailed calculations below.

B. Elasto-optic noise

We can model the WGM volume as a tube of length $2\pi R$ and radius r. We estimate r from $V_m = 2\pi^2 R r^2$, where the mode volume V_m is given by [7] $V_m \simeq 3.4\pi^{3/2}(\lambda/n)^{7/6}R^{11/6}$, where λ is the optical wavelength,

$$r \simeq 0.335(\lambda/n)^{7/12}R^{5/12}. \tag{18}$$

We calculate the strain energy that results from a uniform pressure P applied to the cylindrical surface of the tube, approximating the WGR material as isotropic. Applying the plane-strain condition, the nonzero stresses in the tube are $\sigma_{rr} = \sigma_{\theta\theta} = -P$, $\sigma_{zz} = -2\mu P$, where μ is Poisson's ratio, and the resulting strain energy is

$$U = \pi^2 r^2 R P^2\left[\frac{3}{3\kappa + G}\right], \tag{19}$$

where G is the shear modulus. The applied force is $F = (2\pi)^2 r R P$, and we get

$$\tilde{\sigma}_{dr/r}(\tau) = \frac{\sqrt{6\ln(2)}}{2\pi^3/2}\left[\frac{k_B T\phi}{r^2 R(3\kappa+G)}\right]^{1/2} = 0.55\left(\frac{n}{\lambda}\right)^{7/12} R^{-11/12}\left(\frac{k_B T\phi}{3\kappa+G}\right)^{1/2}, \tag{20}$$

$$\tilde{\sigma}_{\rm EO}(\tau) \simeq 0.55\left(\frac{n^{31/12}}{\lambda^{7/12}R^{11/12}}\right)\left(\frac{k_B T\phi}{3\kappa+G}\right)^{1/2}\frac{p_{11}+2p_{12}}{3}. \tag{21}$$

For a 1-mm-radius resonator, at $\lambda = 1.56$ μm and with $G = 45$ GPa, this numerically evaluates at 5.5 K to 7×10^{-16}, close to the more accurately calculated result below.

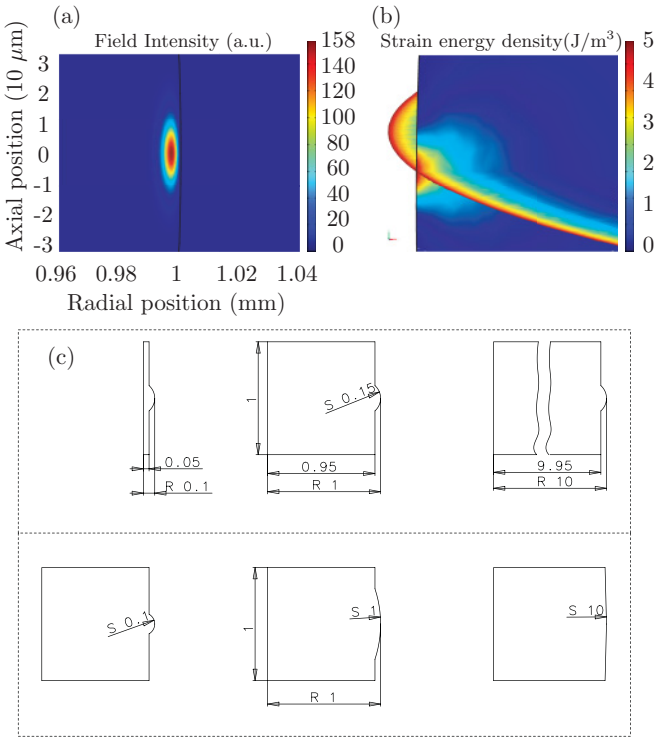

FIG. 1. (Color online) (a) Simulated mode profile of a CaF_2 disk, as shown by the electric field intensity (arbitrary units). The radius (R), surface radius of curvature (S), and thickness are all 1 mm. (b) Simulated strain energy density in the same disk, shown in two orthogonal slices, $\theta = 0$, which shows the strain energy distribution in a cross section of the resonator, and $z = 0$, which shows the strain energy distribution in the resonator-mode-maximum plane. (c) Geometries used for disk simulation.

IV. RESULTS

We perform the calculation for sphere and disk radii ranging from 0.1 to 10 mm, and for disk surface radii of curvature ranging from 0.1 to 10 mm. The disk shapes used are shown in Fig. 1(c). To numerically evaluate the Allan deviation with Eqs. (8) and (14) we must know the material loss angle ϕ. Nawrodt *et al.* [18] measured the Q of mechanical modes of a pure crystalline CaF_2 cylinder as a function of temperature. In the cylinder's fundamental drum mode, material motion is concentrated near the cylinder axis and away from the experimental support. We therefore take the reported Q of the cylinder's fundamental drum mode as representative of the bulk material loss and therefore as the limiting value achievable for losses. The Q of this mode ranged between 10^7 and 5×10^8 in the temperature range 5-300 K. Using this loss angle $\phi = 1/Q = (2 \times 10^{-8}, 5 \times 10^{-8})$ (values at 5 K, 300 K), we obtain the Allan deviation values shown in Table I. Uncertainty in ϕ is the principal uncertainty in our calculation. For different values of ϕ the BB and EO noise terms scale as $\phi^{1/2}$.

TABLE I. Calculated Brownian boundary and elasto-optic noise for CaF_2 spheres and disks at 300 K and 5 K. R denotes radius and S the surface radius of curvature.

R (mm)	S (mm)	σ_{BB} RT	σ_{EO} RT	σ_{BB} 5 K	σ_{EO} 5 K
Spheres					
0.1		2×10^{-14}	9×10^{-14}	2×10^{-15}	8×10^{-15}
1.0		8×10^{-16}	1×10^{-14}	7×10^{-17}	1×10^{-15}
10		3×10^{-17}	2×10^{-15}	3×10^{-18}	1×10^{-16}
Disks					
0.1	0.15	2×10^{-14}	9×10^{-14}	2×10^{-15}	8×10^{-15}
1.0	0.15	9×10^{-16}	1×10^{-14}	8×10^{-17}	1×10^{-15}
10	0.15	5×10^{-17}	2×10^{-15}	4×10^{-18}	2×10^{-16}
1.0	0.1	9×10^{-16}	1×10^{-14}	8×10^{-17}	1×10^{-15}
1.0	1.0	9×10^{-16}	1×10^{-14}	8×10^{-17}	1×10^{-15}
1.0	10	9×10^{-16}	1×10^{-14}	7×10^{-17}	1×10^{-15}

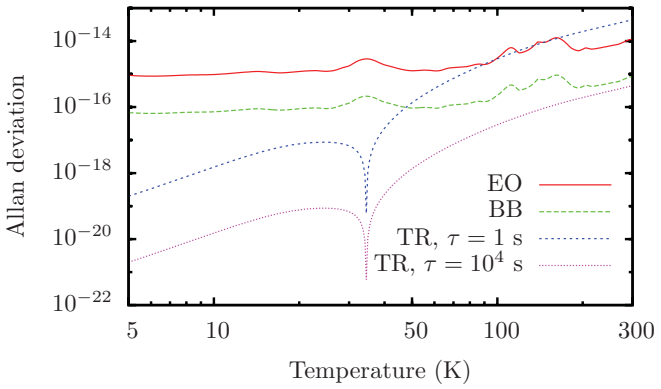

FIG. 2. (Color online) Thermal noise for a 1-mm-radius CaF_2 sphere from 5.5 to 300 K. TR denotes thermorefractive noise, BB Brownian boundary noise, and EO electro-optic noise. There is a zero in the first-order thermorefractive noise at ~33 K due to the zero crossing of dn/dT.

Figure 2 shows the different thermal noise terms for a millimeter-sized resonator. At room temperature and short time scales, the dominant thermal noise contribution is the thermorefractive noise, in agreement with experiments [10,11]. The BB and EO noises vary with temperature as $[T\phi(T)]^{1/2}$, while the temperature dependence of the thermorefractive noise is the much stronger function $T(1/n)(dn/dT)\sqrt{\gamma(T)}$. Thus the BB and EO noise terms become relatively more important with decreasing temperature. The EO noise is an order of magnitude larger than the BB noise for millimeter-sized WGRs, and becomes the dominant noise component at low temperatures and long time scales.

Figure 3 shows the scaling of the calculated noise terms with disk radius and surface radius of curvature. We see that within the range of values considered, the noise is essentially independent of surface radius of curvature, and the ratio of EO to BB noise scales approximately as $R^{0.5}$ ($\sigma_{EO} \propto R^{-0.8}$, $\sigma_{BB} \propto R^{-1.3}$). For a sphere the scaling is similar ($\sigma_{EO} \propto R^{-0.9}$, $\sigma_{BB} \propto R^{-1.4}$). This scaling agrees with the simple estimates in the previous section, for which $\sigma_{EO} \propto R^{-0.9}$, $\sigma_{BB} \propto R^{-1.5}$. The thermorefractive noise depends on mode volume in the same way as does the EO noise, and should thus have a similar dependence on R.

Thus we see that lower noise levels are achieved by going to lower temperatures and larger resonators, with extrapolated noise levels at the 10^{-17} level for a 10-mm-radius sphere at 25 mK and for a 10-cm-radius sphere at 1.7 K, where we have used the 5 K value of ϕ.

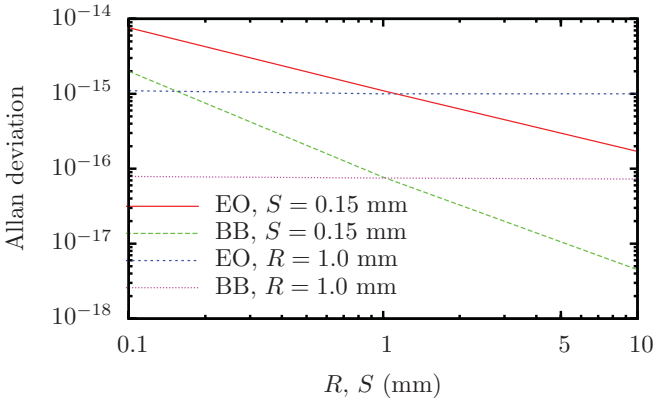

FIG. 3. (Color online) 5.5 K Allan deviation due to Brownian boundary noise and elasto-optic noise of a CaF_2 disk WGM as a function of disk radius R and surface vertical radius of curvature S. BB, $R = 1.0$ mm denotes the Brownian boundary noise as a function of S, for $R = 1.0$ mm. $\phi = 2 \times 10^{-8}$.

V. CONCLUSION

We have calculated the thermal noise limit to the frequency stability of crystalline CaF_2 whispering-gallery resonators set by dimensional fluctuations, by direct application of the fluctuation-dissipation theorem and using the widely applied structural damping model. We have identified a new source of thermal noise in whispering-gallery resonators, due to the elasto-optic effect. This noise is smaller than the thermorefractive noise at room temperature, so it has not been observed in previous room-temperature experiments. At temperatures sufficiently below room temperature (e.g., 50 K), the elasto-optic noise dominates. The total thermal noise is reduced by increasing the resonator size and reducing the temperature. WGRs have already been operated at cryogenic temperatures [19,20], and therefore an experimental study of the noise at low temperatures should be feasible. One important result of such studies will be a determination of the loss angle ϕ, which can at present only be estimated. For achieving

TABLE II. CaF_2 material properties. Property values at intermediate temperatures may be found in the cited references.

Property		Value	Ref.
Refractive index (n)		1.43	[21]
Elastic constants	C_{11}	164 GPa	[22]
	C_{12}	53.0 GPa	
	C_{44}	33.7 GPa	
Thermal conductivity (γ)	300 K	9.71 W m^{-1} K^{-1}	[23]
	5.5 K	1200 W m^{-1} K^{-1}	
Thermorefractive index	295 K	8.4×10^{-6}	[21]
$[\lvert(1/n)(dn/dT)\rvert]$	5.5 K	1.5×10^{-9}	
Loss angle (ϕ)	300 K	5×10^{-8}	[18]
	5.5 K	2×10^{-8}	
Elasto-optic constants:	p_{11}	0.039	[24]
	p_{12}	0.223	
	p_{44}	0.051	
Thermal expansion	295 K	1.89×10^{-5} K^{-1}	[25]
coefficient (α)	5.5 K	6.4×10^{-10} K^{-1}	[a]

[a]Extrapolation from 20 K data using T^3 dependence.

TABLE III. Modeled fundamental electromagnetic modes: sphere.

Sphere radius (mm)	Mode azimuthal index	Mode frequency (10^{14} Hz)	Mode polar intensity $1/e^2$ half-width (μm)
0.1	559	1.9164	4.25
1	5706	1.9152	13.5
10		1.9149	42.0

TABLE IV. Modeled fundamental electromagnetic modes: disk.

Disk radius (mm)	Vertical radius of curvature (mm)	Mode azimuthal index	Mode frequency (10^{14} Hz)	Mode polar intensity $1/e^2$ half-width (μm)
0.1	0.15	559	1.9156	4.6
1	0.15	5706	1.9152	8.2
10	0.15	57320	1.9151	14.1
1	0.10	5707	1.9151	6.7
1	1	5707	1.9151	11.3
1	10	5708	1.9155	13.0

TABLE V. BB noise calculation for CaF_2 spheres. R denotes the sphere radius, w_z is the mode $1/e^2$ intensity half-width, U is the strain energy 10^6 N/m^2 peak load, F is the total force, and $\sigma_{dR/R}$ is the Allan deviation for $\phi = 2 \times 10^{-8}$.

R (mm)	w_z (μm)	U (J)	F (N)	$\sigma_{dR/R}$ at 5.5 K
0.1	4.25	3.2×10^{-13}	0.0047	2.0×10^{-15}
1	13.5	4.4×10^{-11}	0.15	7.2×10^{-17}
10	42.0	5.3×10^{-9}	4.7	2.6×10^{-18}

TABLE VI. BB noise calculation for CaF_2 disks. R denotes disk radius and S the surface radius of curvature.

R (mm)	S (mm)	w_z (μm)	U (J)	F (N)	$\sigma_{dR/R}$ at 5.5 K
0.1	0.15	4.6	3.8×10^{-13}	0.0051	2.0×10^{-15}
1	0.15	8.2	1.9×10^{-11}	0.091	7.7×10^{-17}
10	0.15	14.1	1.8×10^{-9}	1.6	4.5×10^{-18}
1	0.1	6.7	1.3×10^{-11}	0.075	7.9×10^{-17}
1	1	11.3	3.3×10^{-11}	0.13	7.5×10^{-17}
1	10	13.0	4.2×10^{-11}	0.14	7.3×10^{-17}

TABLE VII. EO noise calculation for CaF_2 spheres. w_ρ is the mode radial $1/e^2$ intensity half-width and ρ_0 is the radial position of mode center.

R (mm)	w_z (μm)	w_ρ (μm)	ρ_0 (mm)	U (J)	F (N)	$\sigma_{dr/r}$ at 5.5 K
0.1	4.25	1.1	0.0986	7.1×10^{-14}	0.0088	2.3×10^{-14}
1	13.5	2.5	0.996	4.6×10^{-11}	0.65	2.9×10^{-15}
10	42.0	5.0	9.99	2.3×10^{-8}	41	4.2×10^{-16}

TABLE VIII. EO noise calculation for CaF_2 disks.

R (mm)	S (mm)	w_z (μm)	w_ρ (μm)	ρ_0 (mm)	U (J)	F (N)	$\sigma_{dr/r}$ at 5.5 K
0.1	0.15	4.6	1.1	0.986	8.8×10^{-14}	0.0094	2.3×10^{-14}
1	0.15	8.2	2.5	0.997	1.2×10^{-11}	0.39	3.3×10^{-15}
10	0.15	14.1	5.3	0.999	1.5×10^{-9}	14	5.2×10^{-16}
1	0.1	6.7	2.5	0.997	6.7×10^{-12}	0.31	3.3×10^{-15}
1	1	11.3	2.5	0.997	2.9×10^{-11}	0.53	3.1×10^{-15}
1	10	13.0	2.5	0.997	4.2×10^{-11}	0.61	3.0×10^{-15}

extremely low total noise, it would be favorable to operate large resonators ($R \geqslant 50$ mm) at temperatures $\leqslant$100 mK, where a noise level $\leqslant 4 \times 10^{-17}$ is estimated from the present work.

ACKNOWLEDGMENTS

This work was performed in the framework of project AO/1-5902/09/D/JR of the European Space Agency. We thank J. de Vicente and I. Zayer for support.

APPENDIX A: MATERIAL PROPERTIES

Material properties are presented in Table II.

APPENDIX B: CALCULATION RESULTS

We tabulate here more detailed results of the numerical calculation. Electromagnetic modeling results are given in Tables III and IV. Strain-energy results are given in Tables V–VIII.

[1] H. B. Callen and T. A. Welton, Phys. Rev. **86**, 702 (1951); R. F. Green and H. B. Callen, *ibid.* **88**, 1387 (1952).

[2] K. Numata, A. Kemery, and J. Camp, Phys. Rev. Lett. **93**, 250602 (2004).

[3] Y. Levin, Phys. Rev. D **57**, 659 (1998).

[4] V. B. Braginsky, M. L. Gorodetsky, and S. P. Vyatchanin, Phys. Lett. A **264**, 1 (1999).

[5] F. Bondu, P. Hello, and J.-Y. Vinet, Phys. Lett. A **246**, 227 (1998).

[6] A. Chiasera, Y. Dumeige, P. Feron, M. Ferrari, Y. Jestin, G. N. Conti, S. Pelli, S. Soria, and C. Righini, Laser Photon. Rev. **4**, 457 (2009).

[7] V. B. Braginsky, M. L. Gorodetsky, and V. S. Ilchenko, Phys. Lett. A **137**, 393 (1989).

[8] A. A. Savchenkov, A. B. Matsko, V. S. Ilchenko, and L. Maleki, Opt. Express **15**, 6768 (2007).

[9] A. Matsko, A. A. Savchenkov, N. Yu, and L. Maleki, J. Opt. Soc. Am. B **24**, 1324 (2007).

[10] M. L. Gorodetsky and I. S. Grudinin, J. Opt. Soc. Am. B **21**, 697 (2004).

[11] J. Alnis, A. Schliesser, C. Y. Wang, J. Hofer, T. J. Kippenberg, and T. W. Hansch, Phys. Rev. A **84**, 011804 (2011).

[12] A. D. Ludlow, T. Zelevinsky, G. K. Campbell, S. Blatt, M. M. Boyd, M. H. G. de Miranda, M. J. Martin, J. W. Thomsen, S. M. Foreman, J. Ye, T. M. Fortier, J. E. Stalnaker, S. A. Diddams, Y. L. Coq, Z. W. Barber, N. Poli, N. D. Lemke, K. M. Beck, and C. W. Oates, Science **319**, 1805 (2008).

[13] C. Eisele, A. Y. Nevsky, and S. Schiller, Phys. Rev. Lett. **103**, 090401 (2009).

[14] M. Oxborrow, IEEE Trans. Microwave Theory Tech. **55**, 1209 (2007).

[15] M. Oxborrow, e-print arXiv:quant-ph/0607156.

[16] J. F. Nye, *Physical Properties of Crystals* (Clarendon, Oxford, 1985).

[17] N. M. Kondratiev, A. G. Gurkovsky, and M. L. Gorodetsky, e-print arXiv:1102.3790.

[18] R. Nawrodt, A. Zimmer, T. Koettig, S. Nietzsche, M. Thurk, W. Vodel, and P. Seidel, Eur. Phys. J. Appl. Phys. **38**, 53 (2007).

[19] O. Arcizet, R. Riviere, A. Schliesser, G. Anetsberger, and T. J. Kippenberg, Phys. Rev. A **80**, 021803 (2009).

[20] A. Schliesser, O. Arcizet, R. Riviere, G. Anetsberger, and T. J. Kippenberg, Nat. Phys. **5**, 509 (2009).

[21] D. B. Leviton, B. J. Frey, and T. J. Madison, e-print arXiv:0805.0096, with values below 30 K extrapolated using a T^3 law.

[22] D. R. Huffman and M. H. Norwood, Phys. Rev. **117**, 709 (1960).

[23] G. A. Slack, Phys. Rev. **122**, 1451 (1961).

[24] J. Burnett, Sematech 157 nm Tech. Data Review (2001).

[25] D. N. Batchelder and R. O. Simmons, J. Chem. Phys. **41**, 2324 (1964).